Available online at www.sciencedirect.com
ScienceDirect
Journal of Applied Geophysics 63 (2007) 117 – 134
JOURNAL OF APPLIED GEOPHYSICS
www.elsevier.com/locate/jappgeo

Thermal surface characteristics of coal fires 1 results of in-situ measurements

Jianzhong Zhang [a], Claudia Kuenzer [a,*]

[a] Institute of Photogrammetry and Remote Sensing (IPF), Vienna University of Technology, Gusshausstr. 27-29, A-1040 Vienna, Austria

Received 26 October 2006; accepted 16 August 2007

Abstract

Natural underground coal fires are fires in coal seams occurring subsurface. The fires are ignited through a process named spontaneous combustion, which occurs based on a natural reaction but is usually triggered through human interaction. Coal mining activities expose coal to the air. This leads to the exothermal oxidation of the carbon in the coal with the air's oxygen to CO_2 and – under certain circumstances – to spontaneous combustion. Coal fires occur in many countries world wide – however, currently the Chinese coal mining industry faces the biggest problems with coal fires. Coal fires destroy the valuable resource coal and furthermore lead to many environmental degradation phenomena such as the deterioration of surrounding vegetation, land subsidence and the emission of toxic gasses (CO, N_2O). They additionally contribute to the emission of green house relevant gasses such as CO_2 and CH_4 to the atmosphere.

In this paper we present thermal characteristics of coal fires as measured in-situ during a field campaign to the Wuda coal fire area in south-central Inner Mongolia, China. Thermal characteristics include temperature anomaly measurements at the surface, spatial surface temperature profiles of fire areas and unaffected background areas, diurnal temperature profiles, and temperature measurements inside of coal fire induced cracks in the overlying bedrock. For all the measurements the effects of uneven solar heating through influences of slope and aspect are considered.

Our findings show that coal fires result in strong or subtle thermal surface anomalies. Especially the latter can easily be influenced by heating of the surrounding background material through solar influences. Temperature variation of background rocks with different albedo, slope, aspect or vegetation cover can substantially influence the detectability of thermal anomalies. In the worst case coal fire related thermal anomalies can be completely masked by solar patterns during the daytime. Thus, night-time analysis is the most suitable for thermal anomaly mapping of underground coal fires, although this is not always feasible. The heat of underground coal fires only progresses very slowly through conduction in the rock material. Anomalies of coal fires completely covered by solid unfractured bedrock are very weak and were only measured during the night. The thermal pattern of underground coal fires manifested on the surface during the daytime is thus the pattern of cracks and vents, which occur due to the volume loss underground and which support radiation and convective energy transport of hot gasses. Inside coal fire temperatures can hardly be measured and can only be recorded if the glowing coal is exposed through a wider crack in the overlaying bedrock. Direct coal fire temperatures measured ranged between 233 °C and 854 °C. The results presented can substantially support the planning of thermal mapping campaigns, analyses of coal fire thermal anomalies in remotely sensed data, and can provide initial and boundary conditions for coal fire related numerical modeling.

In a second paper named "Thermal Characteristics of Coal Fires 2: results of measurements on simulated coal fires" [Zhang J., Kuenzer C., Tetzlaff A., Oettl D., Zhukov B., Wagner W., 2007. Thermal Characteristics of Coal Fires 2: Result of measurements on simulated coal fires. Accepted for publication at Journal of Applied Geophysics. doi:10.1016/j.jappgeo.2007.08.003] we report about thermal characteristics of simulated coal fires simulated under simplified conditions. The simulated set up allowed us to measure even more parameters under undisturbed conditions — especially inside fire temperatures. Furthermore we could demonstrate the

* Corresponding author. Tel.: +43 1 58801 12249; fax: +43 1 58801 12299.
E-mail addresses: jz@ipf.tuwien.ac.at (J. Zhang), ck@ipf.tuwien.ac.at (C. Kuenzer).

0926-9851/$ - see front matter © 2007 Elsevier B.V. All rights reserved.
doi:10.1016/j.jappgeo.2007.08.002

differences between open surface coal fires and covered underground coal fires. Thermal signals of coal fires in near range thermal remotely sensed imagery from an observing tower and from an airplane are presented and discussed.
© 2007 Elsevier B.V. All rights reserved.

Keywords: Natural coal fires; Thermal analysis; Temperature profiles; Uneven solar heating; Coal mining; China

1. Introduction

Coal fires are a natural hazard occurring worldwide in countries such as the US, India, Australia, South Africa, China and many more (Glover, 1998; Prakash and Gupta, 1999; Pennig, 2003; Kuenzer, 2005). To a coal fire we refer to as burning volume of coal. This coal can be a burning coal seam exposed to the surface, a burning underground seam or a burning coal waste or coal storage pile. Coal fires can ignite naturally or through human influence, whereas the latter is the cause in most of cases of coal fire ignition (Kuenzer et al., 2007a). Coal ignites through a process called spontaneous combustion. The reaction of carbon in the coal with oxygen in the air is an exothermal process, during which heat is released. If this heat cannot be released from the inner surfaces of a coal volume the coal can ignite at temperatures as low as 80 °C (Banerjee, 1982; Chaiken et al., 1998; Walker, 1999). Conditions, which favor the process of spontaneous combustion are a large coal volume, insufficient ventilation, hot outside temperatures, low coal quality with a high volatile content and high pyrite content, large inner surface of the bulk coal material (e.g. through expansion and shrinking in case of repeated wetting and drying) and mining activity (Bylo, 1960; Banerjee et al., 1972). Although paleo-coal fires burning for hundreds of years are known (Schneider, 1996; Gielisch, 2002) that prove the existence of naturally occurring coal fires, most coal fires existing nowadays are related to mining activities. Mining leads to the exposure of formerly covered coal volumes to the outside air. Mining furthermore leads to the extension of the inner surface of coal volumes and exposes the coal to the anthropogenic risk of accidental ignition through open fire (technical accidents, cigarettes, coal burning for cooking and heating) (van Genderen and Guan, 1997; Rosema et al., 1999; Zhang, 2004; Kuenzer, 2005).

Coal fires lead to the emission of large amounts of green house relevant as well as toxic and health threatening gasses. Due to the volume loss underground coal fires lead to cracks in the overlying bedrock surface and can also cause land subsidence (Chen, 1997). As shown in Figs. 1 and 3 it is through the cracks that hot gaseous emissions of the coal fires reach the surface. Thus coal fire related cracks are dominant structures at which temperatures above underground coal fires are usually highest. Coal fires also lead to the deterioration of vegetation (Rathore and Wright, 1993; Kuenzer and Voigt, 2003), and the endangering of mining activities.

Fig. 1. A typical coal fire in the mining area of Wuda in north central China. Gaseous emission of the burning coal seam underground limit the visibility (left). The co-author is taking a photograph into one of the cracks, which occur due to volume loss underground. This picture can be seen on the right side. The area shown here is about 30 cm high and 40 cm wide. Temperatures measured exceeded 800 °C. Left photo: C. Hecker, 2003, right photo: C. Kuenzer, 2003.

Last but not least they lead to the loss of the valuable resource coal. It is estimated that the loss of coal due to coal fires in China equals the German annual hard coal production (Kuenzer et al., 2007a). The amount of CO_2 released due to coal fires in e.g. China is estimated to contribute with 0.1% to all human induced CO_2 emissions on a global scale (Kuenzer et al., 2007d). Due to these catastrophic environmental and economic impacts the problem of coal fires is addressed in many countries and from various research disciplines.

Coal fires can be extinguished by the depletion of the fire with oxygen (e.g. covering with sand and loess), the cooling of the fire (e.g. water injections), removal of the burning material (coal) as well as the separation of burning areas from unaffected parts of the seam with methods such as underground cement- or colloid barriers.

Numerous authors have addressed the problem of coal fires based on mineralogical, geophysical and remote sensing based research. The first group of researchers is mainly interested in the formation of new minerals around coal fire induced cracks and vents and investigates chemical changes of the coal and surrounding bedrock or facilitates bore hole drillings and geologic mapping to date age, depth and progression of a fire (Lapham et al., 1980; Livingood et al., 1999; Coates et al., 2005; Masalehdani et al., 2005). The second group employs methods such as gas sample analysis, electromagnetic profile measurements, geophysical modeling, temperature measurements, micro seismic, and geoelectrics to quantitatively analyze, locate and predict the coal fires and their development (Lohrer et al., 2005; Wessling et al., 2005; Litschke et al., 2005; Wessling, 2007). Remote sensing based coal fire research has mainly focused on coal fire related thermal anomaly detection (Moxham and Greene, 1967; Fisher and Knuth, 1968; Knuth et al., 1968; Greene et al., 1969; Ellyett and Fleming, 1974; Li, 1985; Mansor et al., 1994; Prakash et al., 1995; Saraf et al., 1995; Giglio et al., 1999; Prakash and Gupta, 1999; Kuenzer et al., 2007b,c) the detection of land cover changes in the mining environments (Prakash and Gupta, 1998), the detection of land surface subsidence due to the volume loss underground (Guan, 1989), and the development of methods for coal fire risk area delineation (Kuenzer, 2005; Kuenzer et al., 2007b). Furthermore, in depth thermal analysis, such as sub-pixel thermal mapping (Zhang et al., 2004), geologic mapping based on emissivity (Schmugge et al., 1991) and coal fire quantification (Tetzlaff, 2004) were pursued.

All the disciplines mentioned above rely on basic knowledge of coal fires, their genesis, their thermal surface expressions in landscape (thermal anomalies, cracks and vents releasing hot gasses), their dynamics over time (expansion, shrinking) as well as ground truth mappings of coal fires (Kuenzer et al., 2005). In this paper we present a detailed study on thermal characteristics of coal fires, based on numerous repeated in-situ temperature measurements during daily solar cycles as well as during night-time for underground coal fires and unaffected background surfaces. All measurements presented in this paper were collected in the year 2002. However, we undertook numerous field campaigns to the same areas in the following three years (2003, 2004, 2005), finding that conclusions derived form the measurements in the first year were also valid and representative for the years thereafter.

So far there has been no publication presenting in-situ thermal surface characteristics of coal fires in such detail. We consider the findings of this paper as a puzzle-stone in coal fire basic research. The objective of this paper is to help to understand the relationships between coal fire induced thermal anomalies and solar heating patterns and to show how difficult it can be to delineate a thermal anomaly from solar heating of background materials. Thus, temperature measurements of background surfaces had to be performed as well The findings are useful for remote sensing research, where thermal anomaly detection in airborne and satellite imagery is commonly performed; but they also have implications for in-situ mapping procedures. These should be performed when temperature contrasts in study areas are highest (night-time or close to sunrise / sunset). This way, the accuracy of spatial in-situ coal fire mapping as presented by Kuenzer et al. (2005) can be improved. Furthermore, it is important for geophysical research to know temperature ranges of thermal surface anomalies, to know the temperature variations of different background materials and to understand the thermal overlap patterns of coal fire induced thermal anomalies and unaffected background temperatures, and furthermore to know inside coal fire temperature as approximated by inside-crack thermal measurements. The findings can here provide valuable input for initial and boundary conditions of numerical (coal fire) modeling. Furthermore, the knowledge gained can help to chose the right settings for similar temperature measurement setups or thermal anomaly mapping campaigns.

This paper is continued by a second paper presenting the results of coal fire simulation experiments under open air simplified conditions as well as results of analyses of thermal expressions of coal fires in ground-based and airborne thermal imagery. The experiment under simplified conditions with simulated coal fires allowed us to measure multiple inside coal fire temperatures, and to gain even more systematic findings under very homogeneous settings, compared to the rather complex in-situ conditions.

2. Study areas and general observations

Fig. 2 shows the location of the study area of Wuda within China (blue box). Wuda is located adjacent to the Yellow River in the south-central part of Inner Mongolia Province.

The north-south striking structural syncline located 5 km west of Wuda has a spatial extent of 35 km^2 and holds an expected total reserve of 630 million tons of coal. The coal layers originate from Upper Carboniferous and Lower Permian times (Dai et al., 2002). Mineable reserves are stated to be 27 million tons with seam thickness varying between 1.5 and 12 m. The coal layers are interbedded in different layers of coarse to fine-grained white to dark grey or yellowish sandstone and grayish-, brown- or green-yellowish shale with varying organic content also originating from the Carboniferous and Permian. Occurring formations are the Taiyuan-, Shanxi-, Xiashihezi- and Shangshihezi formation. The Taiyuan formation is the major coal bearing formation (Dai et al., 2002). The strata dip to the East with an average dip angle of 6 to 10°, but steeper dips occur as well. Quaternary alluvial layers of silt, sand and gravel unconformably cover small parts of the Permian and Carboniferous outcrops (Kuenzer, 2005).

In the syncline area the coal layers have been mined under the authority of the "Wuda Coal Mine Bureau" within the three coal mines of Wuhushan operating in the South, Huangbaici in the East and Suhai-Tu in the Northwest since 1958. In these three mines three different qualities of coal – fatcoal, cooking coal and steam coal – are being extracted from the 17 mineable of the overall 24 coal seams. The upper seven coal seams from Permian times, belonging to the Shanxi group, have an overall thickness of 88 m and are characterized by a low sulfur and a high ash content. All lower seams from the Carboniferous belong to the Thairen group and have a high sulfur and low ash content (Jia, 2002; Sun, 2003; Kuenzer, 2005).

Since commercial mining in the Wuda syncline started in 1958, 120 megatons have been mined by the year 2000. Mainly mechanized longwall methods are applied and the average mining depth of state run- or commercial mines is around 100 m but can reach up to 200–300 m. The first coal fires in the area were discovered in 1961. Before 1989 most coal fires in Wuda were isolated and scattered in different locations. The isolated fires started to connect gradually between 1989 and 1995. An acceleration of the process from year to year is observed. The recent annual amount of coal being burned is estimated to be 200,000 t. It is assumed that so far, over 1 million tons of coal have been destroyed or became inaccessible due to coal fires. In 2002 8.8% of the three coal mining areas in the syncline are affected by coal fires and the coal fire area has an extent of 3.07 km^2 (Jia, 2002).

The fires in Wuda are monitored by mine engineers and mine administrators and have been numbered to provide a common reference. In 2000, an assessment of the boundaries of the coal fires by satellite data, GPS-field measurements and geologic analysis was undertaken by the Wuda mine. Thermal measurements and imaging (see Fig. 3) as well as borehole drillings supported these activities. The result is a map of Wuda syncline with 16 demarcated coal fire areas. These coal fires were subsequently mapped in the following years by a team including the authors. We provided regular reports on the dynamics of the individual fires to the Wuda mining authorities. Results can be found in Kuenzer et al. (2005).

3. Measurement set up in-situ

In September 2002, a field campaign was conducted to the Wuda coal mining area. Coal fire surface anomaly temperatures and surface temperatures for typical background materials (unaffected by coal fires) were measured using a Raytec thermometer and contact thermometers. The Raytec thermometer allowed for highly precise radiant temperature measurements without being in direct contact with the surface. Precision is 0.1 °C of readings up to 900 °C in the 8 μm to 14 μm domain. The contact thermometer has a handle and a 12.8 cm long probe looking like a screwdriver. It measures the kinetic temperature at the head of the probe. The time mentioned in this paper is Chinese Coast Time (CCT, Time Zone 8), which is equal to Greenwich Mean Time plus 8 h (GMT+08:00). Local solar noon time during our measurement campaign in September was 12:47.

The scale of the measurements is defined through our local setups. We measured temperature profiles within areas under 10×10 m. Temperature profiles along cracks or other surfaces were also below 10 m, except in one case, where we measured a 300 m profile. The setups were defined by three factors. Firstly, our goal was to understand thermal patterns in detail and especially investigate thermal anomalies along cracks, which usually have a small extent. Secondly the need to repeat measurements regularly within a diurnal cycle,

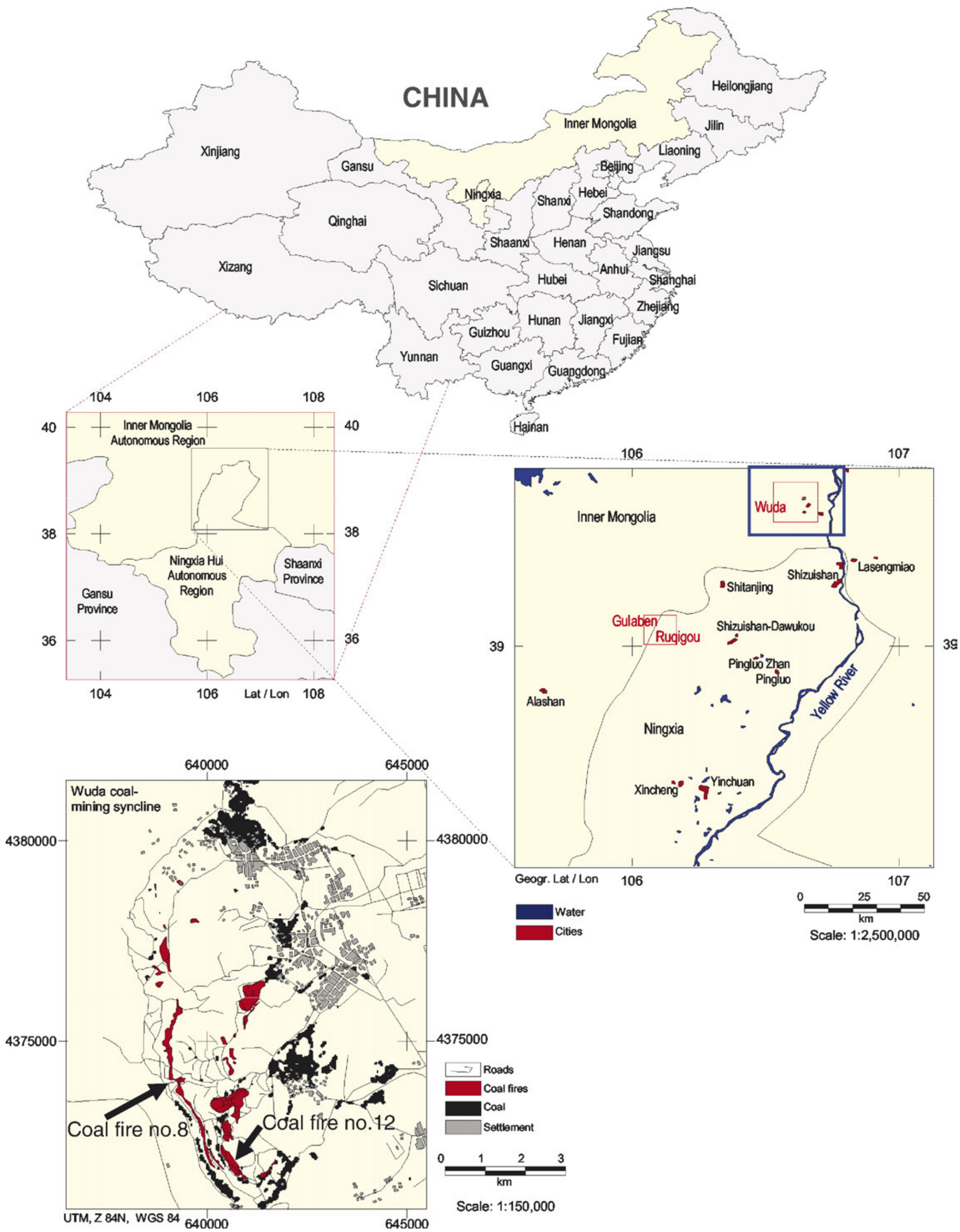

Fig. 2. Location of the study area within China and in more detail. Only the coal fire area of Wuda (blue box in middle figure) was investigated. Note the structural "ear shaped" syncline of Wuda with the 16 coal fires (dark red) at the bottom of the map. Coal fires No. 8 and No. 12 – mentioned in the text – are marked with arrows. The coal fires were mapped subsequently during the years 2000–2005.

which does not allow to travel greater distances and requests to stay within one measuring area. Thirdly, the nature of the coal fire region influences the set up. The working area has strongly subsided and cracked surfaces, sinkholes, cracks and even exposed fire areas. Thus, moving is limited.

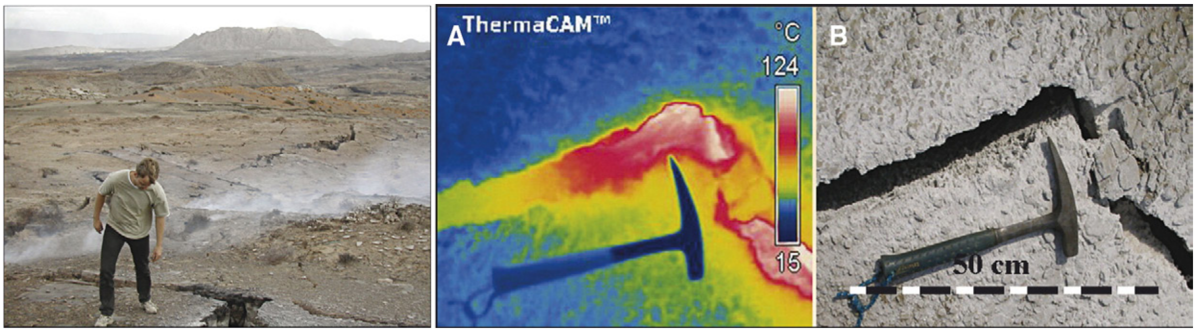

Fig. 3. Underground coal fires in Wuda syncline. Heat is transferred via vents and cracks in the overlying bedrock. Note the gas emissions in the left image. Sudden collapse of bedrock due to the volume loss underground is common. Photo: Kuenzer 2003. The middle image shows a thermal camera picture taken at a crack (right). Tetzlaff (2004).

Measurements were performed along horizontal profiles. Measuring points were clearly defined with 10 cm, 1 m or 10 m distance depending on profile length and measurements over the diurnal cycle were always repeated at exactly the same points. Vertical profiles sub-surface or inside of cracks were performed at centimeter range measuring intervals. All measurements were performed with the same instruments, which were calibrated each morning and showed no discrepancies to the calibration instrument.

To study coal fire related thermal anomalies it is of utmost importance to firstly understand the thermal behavior (such as diurnal temperature patterns, highest and lowest temperatures during day- and night-time, speed of heating etc.) of background materials in the coal fire area. Typical bedrocks and surface covers in our study area include light sandstone, light yellowish desert sand, dark brown shale and coal waste accumulations. Therefore, background temperature measurements were conducted at two representative backgrounds with respect to material, exposition and slope. A light background (sand dune, representing solar patterns of lighter sandy and sandstone surfaces) and a dark background (coal dump pile, representing darker coal dust covered surfaces and dark shale) were investigated.

To analyze the thermal signals of coal fires we measured profiles along coal fire related cracks, where hot gasses are emitted. These cracks are usually the hottest "features" within coal fire areas. Subsurface measurements into the first few centimeters of the soft ground were conducted to investigate sub-surface solar heat progression and the separation of solar and coal fire signals. Vertical inside-crack temperature profiles were conducted to derive temperature gradients and to retrieve direct coal fire temperatures. Furthermore, nighttime profiles orthogonal to cracks, and profiles over a complete coal fire zone were measured.

The following measurements were performed:

- Background temperature measurements of a light background (sand dune) to investigate temperature variation within homogeneous light surfaces depending on aspect, slope and vegetation cover
- Background temperature measurements of a dark background (coal waste pile) to investigate temperature variation within a homogeneous dark surface depending on aspect and slope
- Daytime spatial profiles orthogonal to coal fire related cracks in the bedrock surface to analyze the spatial extent of thermal anomalies
- Daytime vertical subsurface measurements along the crack profiles to investigate heat penetration into the ground within the upper centimeters
- Daytime vertical inside-crack measurements in a wide crack exposing a coal fire to obtain direct coal fire temperatures and vertical heat profiles
- Nighttime temperature measurements above a subsurface coal fire with and without cracks to understand the role of conductive heat transfer
- Large extent profile of a whole coal fire zone including covered, cracked and subsided areas to understand the general temperature patterns at a larger scale

4. Results: thermal characteristics of coal fires

4.1. Field surface temperature measurements of the backround: a sand dune

For background temperature measurements on a representative light sandy surface a small sand dune was chosen. The sand dune is located at the southern part of coal fire No.8 in Wuda coal mine area. (see Fig. 2). Fire No. 8 is one of the largest and most active fires of the nowadays (2007) already 20 underground coal fires in

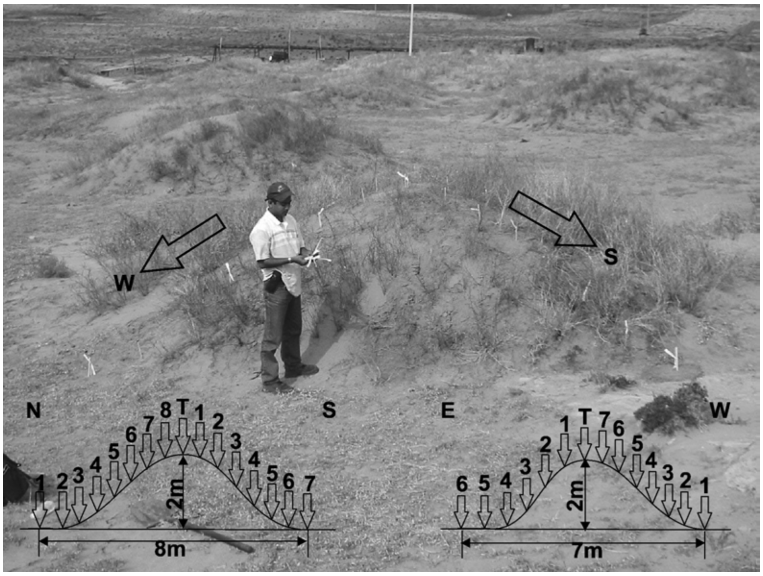

Fig. 4. Setting of measuring points on a sand dune in Wuda coal mine area. N: North; E: East; S: South; W: West; 1–8, T: measuring points. The drawings show the cross section of the sand dune from North to South and East to West. The coordinates for the top of the sand dune are 639403, 4373774 (UTM, Zone 48).

Wuda syncline. The sand dune consists of fine yellow quartz sand. There are bushes growing on it, most of which are dry shrubs (Artemisia family). The sand dune is 2 meters high. From the northern edge to the southern edge, the distance is 8 m. From East to West, the distance is about 7 m. Two measuring lines were marked on the surface of the sand dune: one from North to South and one from West to East. They cross each other on the top of the sand dune. From North to South, there were 16 measuring points, named N1-N8, T and S1-S7. From West to East, there were 14 measuring points, named W1-W7, T and E1-E6. Measuring point T represents the top of the sand dune. The marked measuring points were evenly distributed along measuring lines on the surface. Measuring points N1, S7, W1, E5 and E6 were located at the flat area around the sand dune as shown in the cross sections in Fig. 4. The dip angle for the slope of the sand dune ranges between 30–40°. Temperature measurements of the sand dune are presented in Fig. 4.

Radiant temperatures for each measuring point were recorded every hour on the sunny day of 23rd September 2002. The measurements started at 06:30 before sunrise (06:41) and ended at 19:00 after sunset (18:53). Fig. 5 shows plots of the average temperatures for measuring points N1–N8 plus T (average_N), E1–E6 plus T (average_E), S1–S7 plus T (average_S), and W1–W7

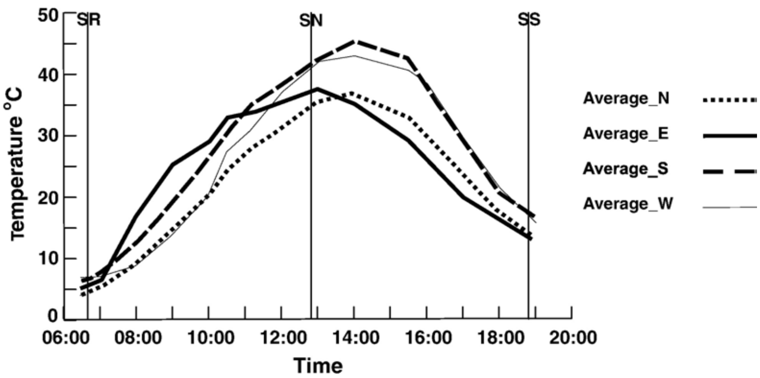

Fig. 5. Average surface temperatures for slopes facing to North, East, South and West of a sand dune in Wuda coal mine area. Average_N: average of temperature measurements for measuring points N1-N8 and T; Average_E: average of measuring points E1–E6 and T; Average_S: average of S1–S9 and T; Average_W: average of W1–W9 and T; SR: sunrise; SN: Solar noon; SS: sunset. The slope facing to the East reaches its highest temperature at 13:00. The slope facing to the North, South and West reach their highest temperatures at 14:00.

plus T (average_W). Average temperatures were calculated according to the arithmetic mean. For example:

$$average\_E = \overline{T_E} = \frac{T_{E1} + T_{E2} + T_{E3} + T_{E4} + T_{E5} + T_{E6} + T_T}{7} \tag{1}$$

where, *average_E*: average temperature for East slope, and T_{E1} to T_{E6} and T_T: temperatures for the measuring points $E1$ to $E6$ and T.

The figure represents the radiant temperature changes between 06:00 to 19:00 for the slope facing to the North, East, South and West respectively. At 6:30 before sunrise, radiant temperatures for each slope show their minimum value ranging from 4 to 8 °C. Temperatures for the slope facing to the East increase from sunrise until 13:00 and then decrease again. The other slopes reach their highest temperature at 14:00. From 07:15 to 11:00, average temperature for the eastern slope is higher than that for other slopes. From 11:00 to 16:00, average temperature of the southern slope is higher than that of the other slopes. From 16:00 to 18:30, average temperature of the western slope has the highest value.

Fig. 6 shows the radiant temperature differences, representing spatial temperature variation in the sand dune. Temperature differences within a slope (here a slope facing East) are calculated according to:

$$E_{\text{diff}} = \text{Max}(T_{E1}, T_{E2}, T_{E3}, T_{E4}, T_{E5}, T_{E6}, T_T) - \text{Min}(T_{E1}, T_{E2}, T_{E3}, T_{E4}, T_{E5}, T_{E6}, T_T) \tag{2}$$

where, E_{diff}: Temperature difference within the eastern slope, T_{E1} to T_{E6} and T_T: temperatures for the measuring points $E1$ to $E6$ and T.

From 07:15, temperature difference within the eastern slope is higher than 5 °C. It reaches its highest value of 20 °C at 09:00. From 07:30, temperature difference within the southern slope is higher than 5 °C. The same applies for the northern slope. Temperature difference within the southern slope reaches its highest value of 16 °C at 13:00, the northern slope shows 14 °C difference at 14:15. From 09:30, temperature difference within the western slope is higher than 5 °C. It reaches its highest difference value of 12 °C at 16:00. The maximum values decrease for the slopes from the East, South, North and West in this order. In the same order the maximum value is shifting to a later time of the day.

Secondly, the temperature difference among slopes A_{diff} (representing the range of temperature values within the entire dune) is calculated from the following equation:

$$A_{\text{diff}} = \text{Max}\left(\overline{T_N}, \overline{T_E}, \overline{T_S}, \overline{T_W}\right) - \text{Min}\left(\overline{T_N}, \overline{T_E}, \overline{T_S}, \overline{T_W}\right) \tag{3}$$

From 07:30 to 18:00, average temperature difference among slopes is higher than 5 °C. The maximum value of 13 °C occurs at 16:00. A_{diff} reaches two peaks at 09:00 and 16:00 due to the slopes facing to the East and West. At 09:00, the eastern slope has a high average temperature and the western slope has a low one. At 16:00, the western slope has a high average temperature and the eastern has a low one.

Thirdly, the temperature differences representing spatial temperature variation in the sand dune T_{diff} was calculated using the maximum value of all the

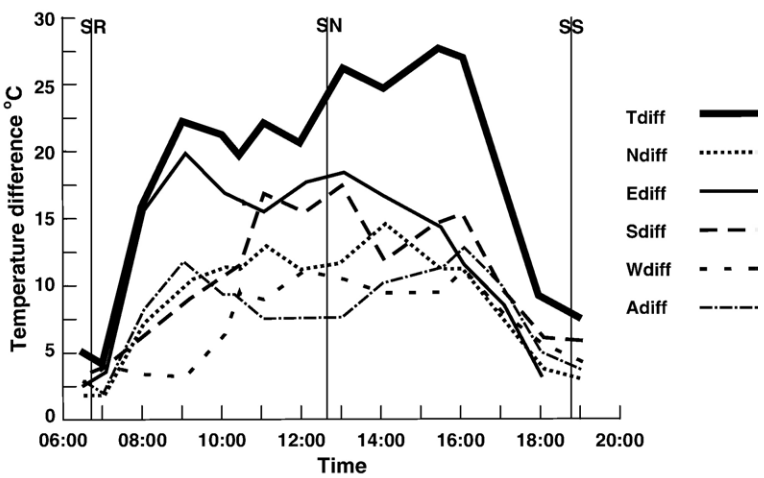

Fig. 6. Surface temperature variation of a sand dune in Wuda coal mine area. SR: sunrise; SN: solar noon; SS: sunset; Ndiff, Ediff, Sdiff , Wdiff: temperature difference within a slope facing to the North, East, South and West; Adiff: average temperature difference among slopes; Ediff: temperature difference in the sand dune. Temperature measurements varied for 28 °C in the sand dune.

measurements minus the minimum value of all the measurements.

$$T_{\text{diff}} = \text{Max}(T_{N1},\ldots,T_{N8};T_{E1},\ldots,T_{E6};T_{S1},\ldots,T_{S7};T_{W1},\ldots,T_{W7};T_T) - \text{Min}(T_{N1},\ldots,T_{N8};T_{E1},\ldots,T_{E6};T_{S1},\ldots,T_{S7};T_{W1},\ldots,T_{W7};T_T) \quad (4)$$

where, T_{diff}: Temperature variation in the sand dune T_{N1},…, T_T: Temperatures for measuring points correspondent with the index. Just about 20 min after sunrise, temperature variance in the sand dune is higher than 5 °C. It has its highest value of 28 °C at 15:30 (measuring point S3 reaches 49 °C while the temperature for E4 is only 21 °C).

Temperature variations among measurements result from topography (slope, aspect), and vegetation influences at the measuring points. Some of them are exposed to the sun, while some of them are shaded by vegetation. At 10:30, when e.g. common earth observing satellites pass over the area, the temperature difference within the sand dune can reach 20 °C; in the afternoon even 28 °C can be reached. This is a higher temperature difference than the difference between many coal fire related thermal anomalies and the background, as it will be presented later in this paper. This is very important to consider when aiming at the daytime extraction of coal fire related thermal anomalies from airborne or space borne thermal–remote sensing data as well as for the mapping of coal fire anomalies in-situ. The measurements show that already a homogeneous surface, which only varies by aspect and slope underlies extreme internal temperature variations. However, underground coal fires under covering bedrock form only very subtle thermal anomalies if no cracks exist for the release of hot gasses. If the coal fire is located too deep underground it is also possible that no conductive heat reaches the surface. These weak anomalies are thus difficult to detect in a terrain with strong temperature variation. The best time to map coal fires in-situ would thus be times when the solar influence is lowest and coal fire thermal anomalies plot strongest against the background. Thus, pre-dawn mappings before sunrise would actually be best. However, to map coal fire areas in the dark is too dangerous and not feasible. Thus the rule applies that mapping shortly after sunrise or close to sunset should be favored. The results also show that for modeling of a coal fire area it is crucial to take the natural settings (aspect and slope of the area, where the coal fire occurs) into account. A thermal anomaly, which can be differentiated against the background will look much different on a south exposed surface than on a north exposed slope.

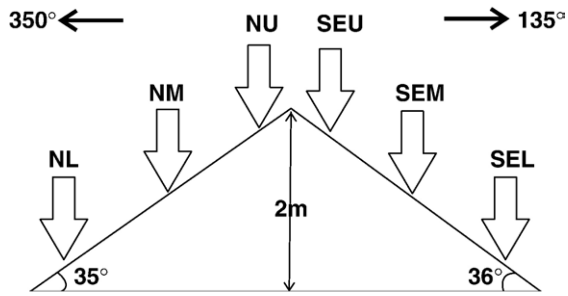

Fig. 7. Setting of measuring points on a coal dump pile in Wuda coal mine area. NL, NM, NU, SEL, SEM, and SEU: measuring points; 350° and 135°: slope dip direction. The top coordinates of the coal dump are 639460, 4373881 (UTM, Zone 48N).

4.2. Field radiant temperature measurements of the background: a coal waste pile

We chose a coal waste pile to investigate temperature variation on a dark background object. Coal waste piles are piles consisting of a mix of low quality coal, bedrock surrounding the coal (in this case black shale or mud stone), and coal dust. Radiant temperatures were measured on the same day as the sand dune. The pile is located 120 m away from the sand dune in NNE direction. Fig. 7 shows that the coal dump pile is about 2 m high and slope angles are about 35°. Three measuring points were set on the slope facing 350°(NNW to N). They represent temperatures for the lower part (NL), middle part (NM) and upper part (NU) of a coal dump pile slope facing north. Another three measuring points were set on the slope facing 135° (SE). They represent temperatures for the lower part (SEL), middle part (measuring point SEM) and upper part (SEU) of a coal dump pile slope facing southeast. Temperature measurements for the measuring points are shown in Fig. 8. So is the temperature difference between the maximum value and the minimum value (Max (NL, NM, NU, SEU, SEM, SEL) — Min (NL, NM, NU, SEU, SEM, SEL)). At 06:50, which is 9 min after sunrise, temperatures for all the measuring points are relatively homogeneous. The difference between the maximum value and the minimum value is 1.6 °C. From 7:15 to 17:00, temperature measurements for the SE slope are higher than that for the N slope. From 10:00 to 14:00, the maximum measurement for the SE slope is over 20 °C higher than the minimum measurement for the N slope. Temperature measurements for all 6 measuring points lie within 5 °C in the time range before 07:00 and after 17:30.

Just like the sand dune (light color, high albedo) the coal dump pile (dark color, low albedo) is a typical

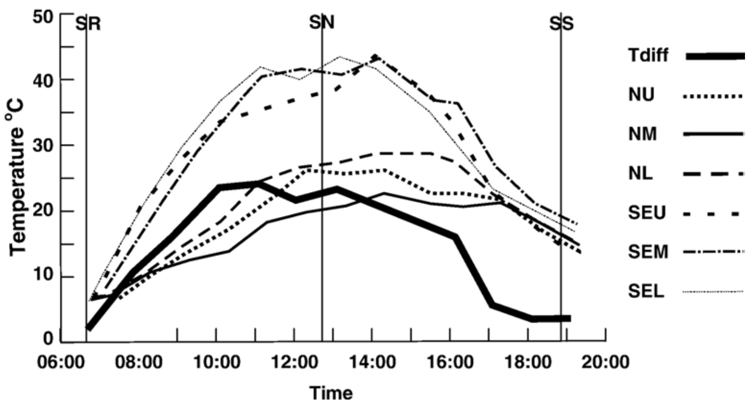

Fig. 8. Surface temperatures and their variation for a coal dump pile in Wuda coal mine area. NL, NM, NU, SEL, SEM, and SEU: temperature for the correspondent measuring point; SR: sunrise; SN: solar noon; SS: sunset; Tdiff: temperature difference.

background surface in the Wuda coal mining syncline. Comparing Figs. 6 and 8 it is obvious that the darker material reaches much higher temperatures during the diurnal cycle than the lighter material. Heating rates (speed of heating) are also higher for a dark material. Temperature differences for the two surfaces cannot be compared, since the sand dune was vegetation covered, while the coal dump pile was bare. Vegetation leads to shadowing and cooler temperature even shortly after sunrise. However, also for the coal dump pile temperature variation within the object could exceed 20 °C, while it is much lower around sunrise and sun set. This again underlines that thermal anomaly mapping is best performed during these times (in case pre-dawn mapping is not feasible). For coal fire thermal anomaly analyses we can furthermore conclude that thermal anomalies at cracks located within a dark surface will be overprinted (masked) earlier by solar influences than if the crack was located within in a bright surface, which heats slower.

4.3. Field temperature measurements of coal fire related cracks

A coal fire related crack, 30 meters north of the sand dune, was chosen as a representative coal fire related thermal anomaly for studying radiant temperature changes during a day. The crack is about 3 m long, 40 cm wide and 2 m deep. It strikes to the NW. At the bottom of the crack, the coal fire is burning; a red flame can be seen. The bedrock around the crack is covered by the same yellow fine sand forming the sand dune. A NE trending measuring line was defined as shown in Fig. 9. From the crack to the SW, there were 6 measuring points named SW1, SW2, SW3, SW4, SW5 and SW6. From the crack to the NE, there were 10 measuring points named NE1, NE2, NE3, NE4, NE5, NE6, NE7, NE8, NE9, and NE10. Locations were marked to ensure that every time the measurements were taken at the same spots. The coordinates for the measuring point NE10 are 639399, 4373749 (UTM, Zone 48). Radiant temperatures for each measuring point were recorded in the same way and on the same day as for the sand dune.

During the measurements we found that between 06:30 to 19:00 the radiant temperature of the fire at the bottom of the crack (measuring point C) has the highest temperature of 239 °C and the lowest of 233 °C, with an average of 237 °C, and a standard deviation of 1.56 °C. It is relatively stable during the day. From 06:30 to 14:00 (see Fig. 9), temperatures for other measuring points increase from 6 °C to 43 °C. Past 14:00 they decreased again.

The measuring points SW1, SW2, SW3, NE8, NE9 and NE10 are taken as background to compare temperature differences between coal fire affected and unaffected areas (see Fig. 9 lowest figure). The temperatures higher than the background are regarded as thermal anomalies. Fig. 9 shows that the width of the thermal anomaly is 3.8 m, 3.8 m, 3.8 m and 4.1 m at 07:00, 09:00, 11:00 and 13:00 respectively if we measure the anomaly extent based on temperature thresholding. Strictly speaking at a sampling interval of 1 m we can only give anomaly extents at this scale, thus the anomaly covers a width of 4 m. Fig. 9 (middle) shows that the width of the thermal anomaly (in this case) does not change substantially as the background temperature increases. The maximum temperature difference between the crack and the background occurs predawn (Fig. 9, upper, 6:30). Over the whole measured diurnal cycle the thermal anomaly does not extend more

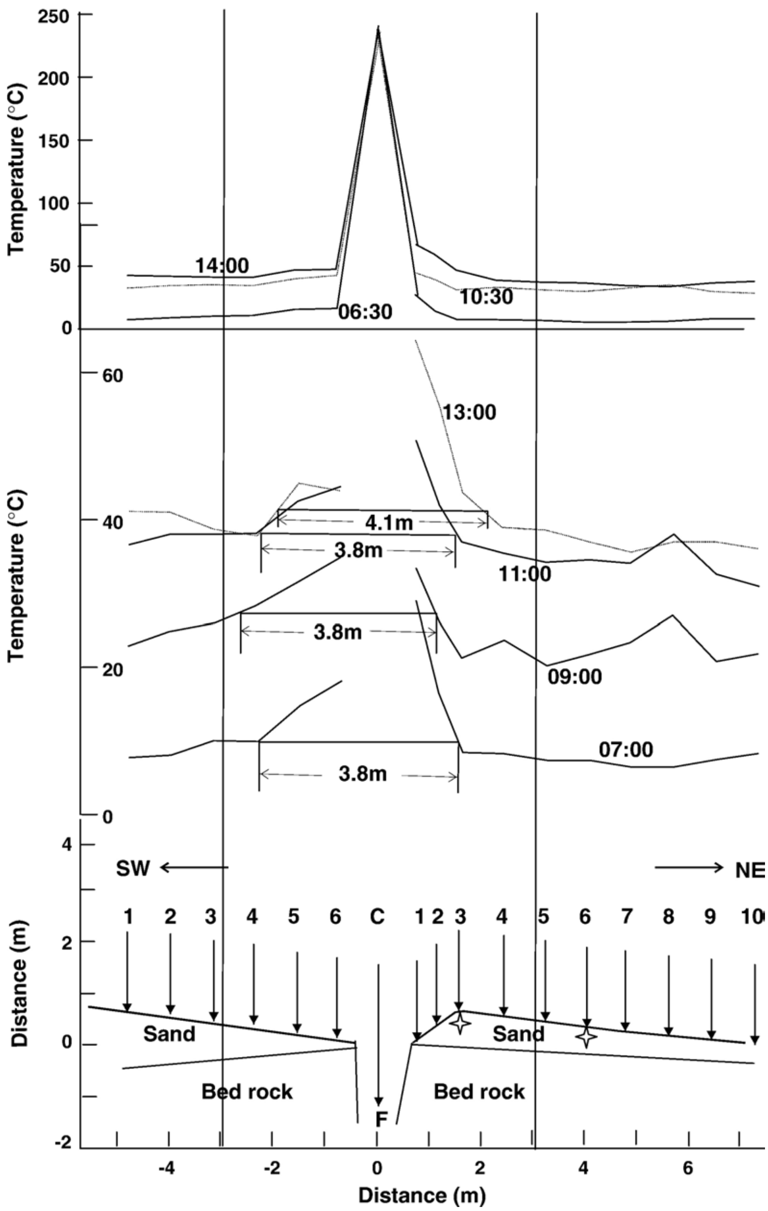

Fig. 9. Surface temperatures for a crack in Wuda coal mine area. Lower: setting of measuring points; C: crack; F: fire; 1–10: measuring spots; middle and upper: temperature profiles. Middle shows only the lower temperature range of the upper figure. The temperatures for the crack (top) are relatively stable during the day. The thermal anomaly does not extend more than 3 m from the crack (inside of the two marking lines). The width of the surface thermal anomaly does not decline as the background temperature increases. The two stars mark measuring point NE3 and NE6 mentioned in the text as well as in Fig. 10.

than 3 m from the crack (to both sides). This can be seen if we look at the extent of the thermal anomaly in all 3 graphs of Fig. 9.

Additionally, temperatures at different depths for measuring point NE3 and NE6 (marked with star in lower part of Fig. 9) have been measured using a contact thermometer three times at 07:30, 09:30, and 11:30. A mark was given at every quarter of the probe and then pressed into the sand until the mark. The readings on the handle represented temperatures below the surface at the depth corresponding to the mark. Measurements include the temperature on the surface, and 1 cm, 3.2 cm, 6.4 cm, 9.6 cm, 12.8 cm below the surface as shown in Table 1 and Fig. 10.

Table 1
Temperature (°C) for different depths at measuring points NE3 and NE6

Measuring point	NE3	NE6	NE3	NE6	NE3	NE6
Start time	7:29	7:34	9:31	9:41	11:25	11:30
Surface	10.1	12.7	26.2	28.7	38.3	35.7
−1 cm	11.9	13.5	25.6	26.5	36.0	34.3
−3.2 cm	19.5	16.7	24.6	22.5	32.1	28.7
−6.4 cm	23.1	18.7	25.0	22.0	29.8	26.8
−9.6 cm	26.0	21.0	26.7	22.2	29.9	25.9
−12.8 cm	27.1	22.7	29.8	23.0	31.5	25.7
End time	7:33	7:40	9:39	9:48	11:29	11:36

Black and white table online and in print.

Measuring point NE3 is about 1 m away from the crack and NE6 is about 3.5 m away from the crack as shown in Fig. 9. Temperatures for 12.8 cm below the surface at NE3 are 5–7 °C higher than that at NE6. The transfer of heat therefore does influence the near surface temperature. Its gradient in this crack system is about 2.4 °C per meter. However, no conclusions can be drawn if the transfer is mainly influenced by convection of hot gasses or conduction through the solid matter.

At 07:30, temperatures from −12.8 cm to the surface at both NE 3 and NE6 were decreasing. On the surface, according to the trend, the temperature for NE6 is supposed to be lower than that for NE3, but the measurements show the opposite, which is due to uneven solar heating. The surface plane, where NE3 is located, is relatively flat. The surface plane, where NE6 is located, has a dip angle of 7° and dip direction of 50° (facing to NE). NE6 thus receives stronger solar heating in the morning. Only 1 hour past sunrise, a thermal anomaly formed 1 m away from the coal fire crack, was affected (masked) by uneven solar heating. This can be observed in Fig. 10, where the surface radiant temperature of NE6 is higher than of NE3 — even though NE3 is much closer to the fire. This finding demonstrates the complexity of coal fire related thermal anomaly patterns, where the border between thermal anomaly and background (or solar masking) is influenced by numerous factors, such as surface material, vegetation density, slope angle and aspect of a measuring point.

At 09:30, temperatures from –12.8 cm to –3.2 cm at NE3 decrease. Temperatures from −3.2 cm to the surface increase. After 3 h past sunrise, the heat from the sun reaches at least 3.2 cm below the surface at NE3. Since NE6 receives more irradiance than NE3, heat reaches 6.4 cm below the surface at the same time. This also demonstrates that solar heat penetration is strongly influenced by slope and aspect.

At 11:30, temperatures from −12.8 cm to the surface at NE6 decrease. Heat from the sun at NE6 reaches at least 12.8 cm below the surface. It reaches −6.4 cm at NE3. On the surface, the temperature for NE3 is higher than that for NE6, which is probably due to the SW wind, transporting the heat from the crack to NE3. Thus, only 5 h after sunrise the solar influence manifests already at a depth of over 12 cm. From Fig. 10 we can conclude that each measuring point in depth is influenced by the coal fire heat from underground and a solar signal from the surface. For graphs with continuous temperature behavior (3@7:30 and 6@7:30), where temperature is always increasing with depth, the profile is solemnly influenced by the coal fire. Of course at coal fire unaffected soils very early in the morning also a temperature increase with depth can be marked — however, not at the rates presented here (over 10 °C within 13 cm). Curves, which show ambiguous temperature behavior (e.g. first temperature decrease with depth, then again increase) like point 6 at 9:30 are influenced by the solar signal at the surface layers and the coal fire in the lower parts. Point 6 at 11:30 does not show any temperature increase with depth anymore, which means that the solar influence has already reached that depth.

Temperatures for another crack, located at coal fire No. 8 in Wuda coal mine area, were measured two times on September 10 and 14, 2002. Fig. 11 shows that the crack is located in a brownish yellow solid sand stone layer. The crack's width (aperture) is about 1m. The wide crack enabled us to use a radiant thermometer to

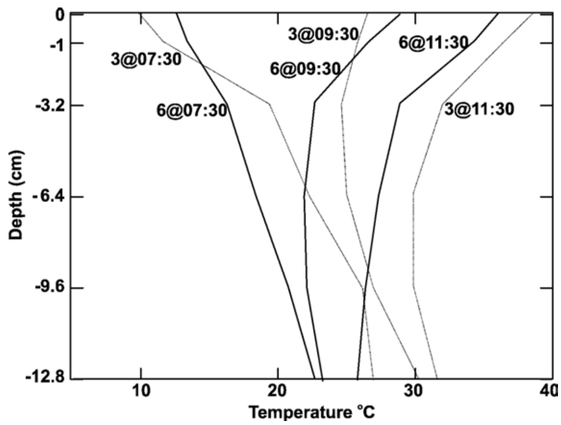

Fig. 10. Underground temperature at measuring points NE3 and NE6. A@B: at measuring point A and time B. One hour after the sunrise, the thermal anomaly formed 1 m away from the coal fire related crack was influenced (masked) by uneven solar heating. At NE3, heat from the sun reaches 3.2 cm below the surface at 09:30 and 6.4 cm at 11:30. At NE6, heat from the sun reaches 6.4 cm below the surface at 09:30 and more than 12.8 cm at 11:30. Measurement accuracy 0.1 °C. Measurements were repeated the next day and show similar patterns.

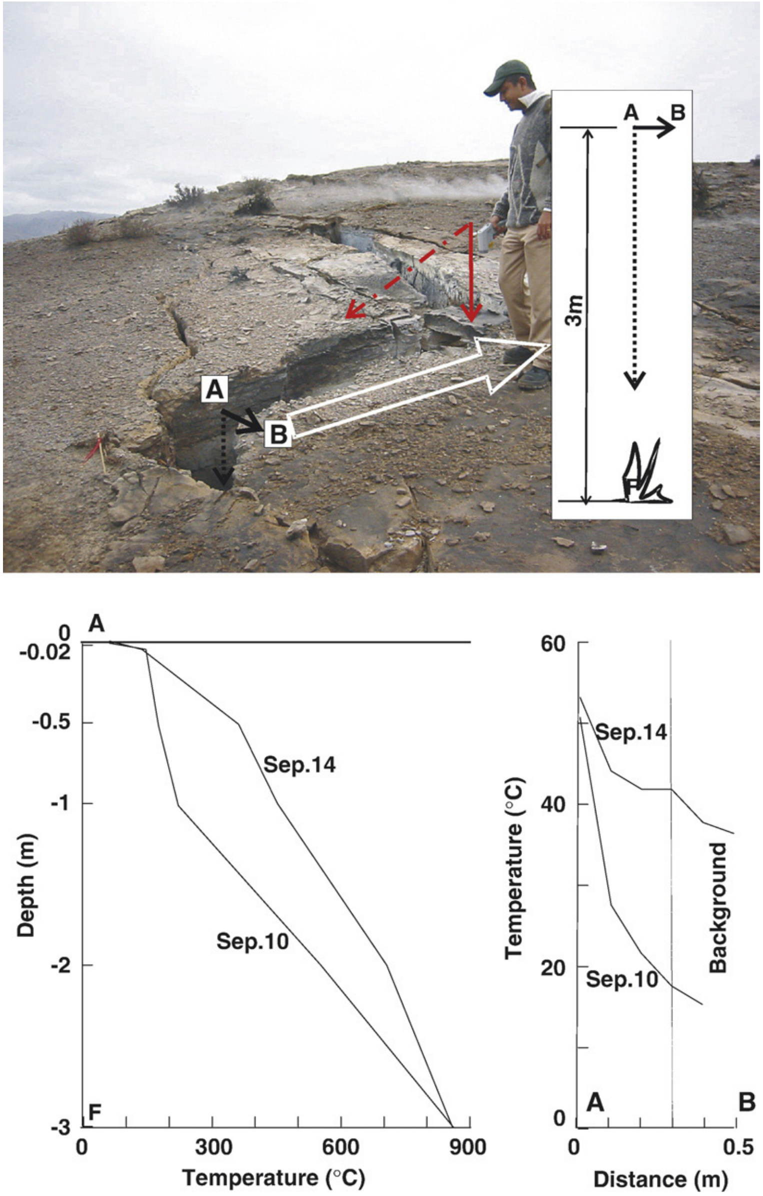

Fig. 11. Temperature profile for a crack at coal fire No. 8, Wuda coal mine area (measured on September 10 and 14, 2002). From −0.02 m to the surface, temperature drops rapidly. On the surface 0.3 m away from the crack temperatures drops to the normal background level. Red arrows indicate the measuring direction of the radiometer: stepwise along the wall of the crack subsurface (dashed) and directly down onto the glowing coal.

measure temperatures from the surface of the crack all the way down to the underground coal fire. The coal fire was burning 3 m below the surface. A vertical temperature profile for the crack is shown in Fig. 11. The measuring points for the vertical profile were taken from the edge of the crack at the following spots: surface, −0.02 m, −0.5 m, −1 m, −2 m below the surface, and at the coal fire (−3 m) itself. The measurements for the coal fire (−3 m) were 850 °C on Sep.10 and 854 °C on Sep.14. Temperatures at −0.02 m below the surface were 139 °C on Sep.10 and 132 °C on Sep.14. At −0.02 m on the edge of the surface, temperatures dropped rapidly to 60 and 66 °C. This horizontal temperature profile at point A for the crack is shown in Fig. 11. From these measurements we can conclude that firstly coal fire temperatures can be measured more or less directly if the glowing coal is exposed through an open crack. Coal fire temperatures can exceed 850 °C. Secondly, temperature from the fire to the surface layer decreases more or less constantly, but shows a very abrupt decrease at the upper 2 cm close to the surface. This sudden decrease is most likely resulting from the influence of cooling wind in the exposed landscape of our study area. However, quantitative wind speed measurements were not undertaken. Furthermore, it is obvious that the extent of the recognizable anomaly does not vary substantially even with slightly varying background temperatures. However, from Fig. 11 we can also see that the extent of the anomaly would slightly increase if background temperature would drop rapidly (e.g. 0 °C snow cover).

Additionally to the vertical profile, temperatures were measured on a horizontal profile between points A (crack at the surface) and point B located 0.5 m away from the crack. From temperature measurements along this horizontal profile at 2 days, it was found that only after about 30 cm the temperature measurements dropped to the normal background temperature, which was 18 °C on Sept. 10 measured at 9:30 and 42 °C on Sept 14 at 13:30.

4.4. A night-time temperature profile on coal fire No.12

Fig. 12 shows a temperature profile on coal fire No. 12, whose coordinates are 640894, 4371674 (see also Fig. 2). The subsurface fire is located below a dense layer of solid sandstone. The measurements were taken at 21:55 on Sep.12. The fire was burning 2 m below the surface in the marked area (F) with a temperature of about 550 °C. This temperature could be retrieved through a measurement in adjacency to the profile, where the fire is exposed on a vertical slope. A crack is located in 5 m distance from the coal fire. The temperature at the bottom of the crack was 206 °C, on the surface it was 46.2 °C. Radiant temperature for a spot in 0.1 m distance from the edge of the crack is 30.2 °C. It can be seen that the underground coal fire does form a thermal anomaly above the covering rocks on the surface as shown by the dotted line in Fig. 12. Since the overlaying bedrock is solid undisturbed sandstone this means that heat can be transferred by conduction from the source of the fire, elevating temperatures only slightly. If convection would play the major role at this spot, firstly, the overlaying bedrock would have to be highly permeable or cracked, and secondly the temperature would have to be much higher. It is known that heat conduction is a slow process compared to convection. Hence, whether or not the heat can reach the surface of the covering bedrock and cause a thermal anomaly depends on the depth and the volume and progression rate of the coal fire in question. If the coal fires are very shallow, they may cause thermal anomalies on the surface of the covering bedrock areas. If the coal fires is burning in a very thick coal seam and progresses slowly (so that the heat source is located in one spot for a longer time), the heat can be transferred to the surface by conduction also. In addition, heat can also transfer laterally from the cracks of higher temperatures to the covering bedrock as presented before. In this case the thermal anomalies will increase in size when a coal fire grows older. This observation is consistent with the thermal modeling results of Wessling (2007). In our case,

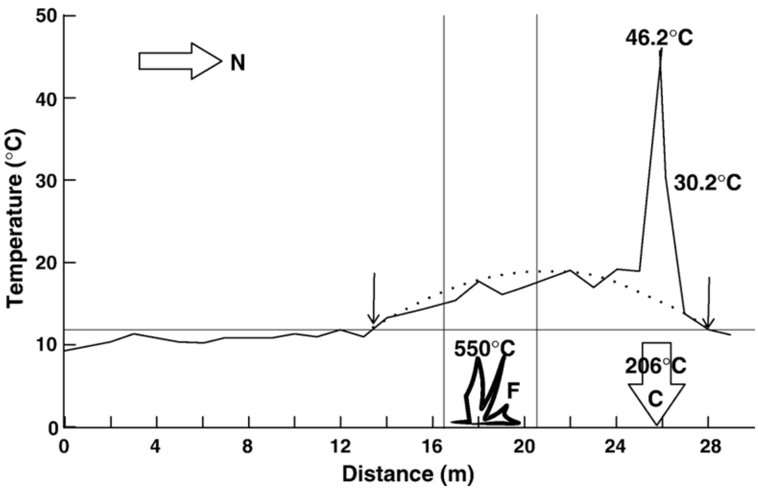

Fig. 12. A temperature profile on coal fire No. 12, Wuda coal mine area (measured at 21:55 on 12 September 2002). The underground coal fire forms a thermal anomaly above the covering bedrocks on the surface as indicated by the dotted line (just a graphic representation). The solid line represents the real temperature measurements. Temperature measurement of 550° results from an exposed area of the fire along a vertical wall in the vicinity of the crack presented above.

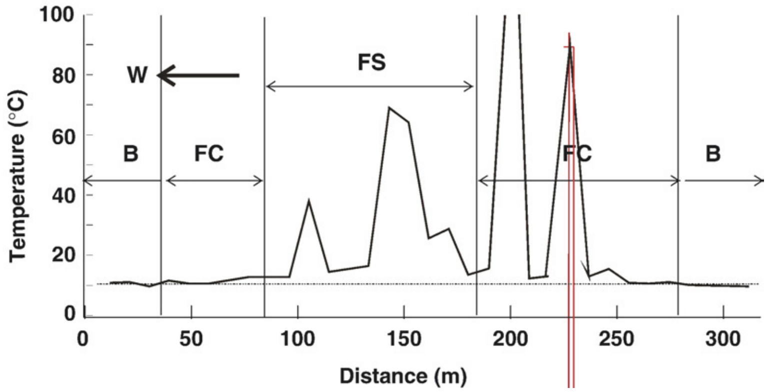

Fig. 13. A temperature profile on coal fire No. 8. B: background; FC: fire area with cracks; FS: fire area with surface subsidence. High surface temperatures for an underground coal fire can be measured only at cracks or close to cracks. In this highly cracked and subsided area, which is dangerous to map measurement intervals could not be chosen equally dense and temperature measurements could not be performed very close to the cracks (e.g. right FC area).

the background temperature is about 12 °C and the thermal anomaly reaches about 20 °C. The temperature difference reaches 8 °C. It is important to note that during the daytime, this thermal anomaly would disappear (be masked) due to the high temperature of the background as discussed before. This demonstrates that weak coal fire anomalies (especially conductive anomalies) can usually not be detected during the daytime.

4.5. A temperature profile on coal fire No.8

Fig. 13 shows a temperature profile on coal fire No.8 measured at 10:00 on September 12th 2002. The profile includes a background part and a coal fire area. Coal fire No.8 consists of two parts. One is an area with multiple cracks but no subsided regions. The other is part consists of many collapsed overlaying bedrock fragments. A lot of cracks exist in this collapsed area. They form a ventilation system for the fire, through which heat is released and new oxygen is received to fan the fire. In Fig. 13 we have background areas (B), where no cracks occur and where radiant temperatures seem not to be influenced by the fire. Fire areas with cracks (FC) show no elevated radiant temperatures for the western part, while in the eastern part (between 180 m and 280 m) there are two outstanding thermal anomalies. The subsidence area (FS) also shows two strong anomalies. It must be mentioned here that the strongly fractured and collapsed area was very dangerous to investigate and thus temperature measurements could not be performed at very dense or equal sampling interval. Thus the seaming spatial extent of the anomalies is not the real spatial extent of the anomalies. Reason for the fact that the western FC area shows no elevated temperatures can be manifold. However, for this area we know that here the coal fire is not active anymore. Otherwise one explanation could be the fact that the hot gasses are escaping via the subsided region.

The observations again underline the complexity of the near-chaotic system of coal fires. While lower temperature anomalies are expected over fully covered fire areas (where conduction is the main source of heat transfer from fires close beneath the surface), stronger anomalies are expected at cracks. However, Fig. 13 has shown that even some cracked areas do not lead to elevated radiant temperature, which can be due to the activity state of the fire or the complex interplay of the underground ingoing and outgoing ventilation pathways.

5. Conclusions

From the interpretation of the different measurements performed on in the coal fire area we can derive the following conclusions:

1. Based on investigation of typical temperature patterns of background surfaces in the coal fire area we found that radiant temperatures on a sparsely vegetated light sand dune can vary for around 28 °C between sunrise and sunset. In a coal dump pile, representing a dark surface, temperatures for a slope facing Southeast were 20 °C higher than that for a slope facing North between 10:00 to 14:00. These temperature differences (variation) caused by uneven solar heating due to different albedo, slope, aspect and vegetation cover can mask thermal anomalies related to coal fires. This is especially important when trying to detect coal fire related thermal signals in airborne or space borne remotely sensed imagery, or when mapping coal fires in-situ. Night-time and especially pre-dawn data (or mapping) would thus be

most suitable for fire mapping and to distinguish the fires against their background. If these are not feasible (often too dangerous) times around sunrise or sunset should be chosen for mapping activities. At those times background internal temperature variation is much less accentuated – in our case it was only 5 °C for the dark surface.

2. During daytime thermal anomalies did not extend for more than 2–3 m from the observed hot cracks (2 m and 0.3 m for the two crack systems investigated). For those very high temperature cracks (233 °C and 854° in the crack center) the extent of the high temperature anomalies actually stays more or less the same during the day as well as with different background temperature. Here the temperature difference is simply too big (the anomaly too strong) as that the background changes would substantially change the extent of the anomaly. However, if background temperature would be very low (e.g. around 0 °C) the extent of the thermal anomaly will seemingly increase slightly. We conclude that especially during daytime, the thermal pattern above an underground coal fire actually is the pattern of cracks and vents in the covering bedrock surface. Hot gasses/water vapor released through cracks and vents contribute much more to detectable coal fire related surface anomalies than conductive heat. The latter can hardly be observed and is thus of no help for daytime coal fire detection in-situ or within thermal imagery.

3. Nighttime measurements above an underground fire covered with solid sandstone show that also conductive thermal anomalies can be mapped if the contrast against the background is big enough. Anomalies occurring through slow conduction of heat through a solid bedrock layer are usually very weak. The anomaly could not be detected during the daytime, since it is overprinted by solar effects. This demonstrates again that coal fire related anomalies are best mapped during times of low solar influence. Also for weaker crack related anomalies it was shown that they were masked only shortly after sunrise. Physically speaking the width of the coal fire expression will not decline as the background temperature increases — it is simply masked. However, it is not occurring as a thermal anomaly any more. Thus, weaker anomalies are much stronger influenced by uneven solar heating than strong anomalies and change their extent over the solar cycle. This can lead to different results if coal fire induced thermal surface anomalies are mapped spatially (as polygons).

4. Vertical kinetic temperature profiles in subsurface showed that one hour past sunrise, a thermal anomaly 1 m away from a coal fire crack was masked by the effects of uneven solar heating. After two hours heat from the sun can reach 3.2 cm below the surface. Presenting underground temperature profiles for points in different distance to a coal fire related crack demonstrated that some points are (up to the surface) influences by coal fire heat exclusively, while others are influenced by solar patterns at the surface layer and coal fire influences in the deeper layer. Also here aspect and slope of the points plays a crucial role for the depth of heat penetration from the surface. This also means that slow conductive heat underground can be masked by solar heating, penetrating into the subsurface during the day.

5. Direct coal fire temperatures could be retrieved at cracks, where direct access to the glowing coal fire was given. Temperatures ranged between 233 °C and 854 °C for inside crack measurements. Even on the surface of cracks temperatures >500° were measured. However, the majority of active cracks release gasses of 100–200 °C.

6. Measurements above a 300 m long horizontal profile over a complete coal fire zone demonstrated the variability of thermal patterns depending on the characteristics of overlaying bedrock. Heavily cracked surfaces lead to strong thermal anomalies, while subsided areas lead to slightly weaker (but still high) anomalies. Unfractured areas usually show now elevated thermal signals during the day. For areas, which are cracked, but do not show elevated temperature the fire has usually burned out and progressed to other areas.

The very extensive database of all the measurements presented in this paper as well as many additional measurements can be found in tabular form in Zhang (2004).

As a last statement we would like to mention that we learned from over 6 years of field work that a big uncertainty in coal fire analysis is the relatively high dynamic of individual fires over short periods. Here high dynamic refers to the rapid growth or shrinking of fires, spontaneous ignition of new fires or even not-understood spontaneous extinction. Depending on coal supply, ventilation, new crack generation and also local weather conditions coal fires can change their burning intensity relatively fast (within days). A frequent monitoring of the fires is of utmost importance when aiming at the extinction of newly ignited or uncontrollably accelerating fires. Thus, knowledge about coal fires and methods to analyze and quantify the fires is a pressing need. The extinction of fires – and the resulting reduction of green-house relevant gaseous emission – shift more and more into the focus of attention of energy companies interested in certified emission trading.

Acknowledgements

The authors thank the numerous German and Chinese partners of the Sino-German Coal Fire Research Initiative lead by DLR for the fruitful collaboration during the past years. We furthermore thank the reviewers for many valuable comments, which improved the quality of the manuscript. Special thanks go to Prof. Wolfgang Wagner (Vienna University of Technology) for his constructive inputs to the manuscript.

References

Banerjee, S.C., 1982. A theoretical design to the determination of risk index of spontaneous fires in coal mines. Journal of Mines, Metals and Fuels vol. 30, 399–406.

Banerjee, S.C., Nandy, D.K., Banerjee, D.D., Chakravorty, R.N., 1972. Classification of coal with respect to their susceptibility to spontaneous combustion. Transactions of the Mining and Metallurgical Institute of India vol. 59 (2), 15–31.

Bylo, Z., 1960. The role of sulphonation in the sponatneous ignition of coal. Serie des Sciences Techniques vol. 8 (2), 107–114.

Chaiken, R.F., Brennan, R.J., Heisey, B.S., Kim, A.G., Malenka, W.T., Schimmel, J.T., 1998. Problems in the control of anthracite mine fires: a case study of the Centralia Mine fire. Report of Investigations 8799 of the United States Department of the Interior. –Pittsburgh, USA, 68. pp.

Chen L., 1997. Subsidence Assessment in the Ruqigou Coalfield, Ningxia, China, using a Geomorphological Approach. Master thesis at ITC, Enschede, Netherlands, pp. 130.

Coates, D.A., Heffern, E.L., Naeser, C.W., Reiners, P., 2005. Coal bed fires — a long history of burning and change in the Northern Great Plains. Proceedings of the International Conference on Coal Fire Research, 29.11.-01.12.2005 Beijing, pp. 98–101.

Dai, S., Ren, D., Tang, Y., Shao, L., Li, S., 2002. Distribution, isotopic variation and origin of sulfur in coals in the Wuda coalfield, Inner Mongolia, China. International Journal of Coal Geology 57, 237–250.

Ellyett, C.D., Fleming, A.W., 1974. Thermal infrared imagery of the Burning Mountain coal fire. Remote Sensing of Environment vol. 3 (1), 79–86.

Fisher, W., Knuth, W., 1968. Detection and delineation of subsurface coal fires by aerial infrared scanning. Geological Society America vol. 115, 67–68.

Gielisch, H., 2002. Loeschung von Kohlebraenden – Statusbericht zum GTZ Projekt. Internal unpublished report of the DMT (German Montan Technology) on a project on coal fire extinction in China within the framework of a German GTZ project, 52. pp.

Giglio, L., Kendall, J.D., Justice, C.O., 1999. Evaluation of global fire detection algorithms using simulated AVHRR infrared data. International Journal of Remote Sensing vol. 20, 947–1985.

Glover L., submitted for publication. Burning Beneath the Surface, Tribune Review, May 3, 1998, Tribune Review Publishing, USA.

Greene, G.W., Moxham, R.M., Harvey, A.H., 1969. Aerial infrared surveys and borehole temperature measurements of coal mine fires in Pennsylvania. Proceedings of the 6th Symposium on Remote Sensing of Environment, University of Michigan, 13-16 October 1969. Institute of Science and Technology, University of Michigan, USA, pp. 517–525.

Guan, H., 1989. Applications of remote sensing techniques in coal geology. Acta Geologica Sinica vol. 2, 253–269.

Jia, Y., 2002. Personal interviews during the fieldwork campaign in September 2002. (Y. Jia is the chief engineer of the coal fire fighting team Wuda).

Knuth, W.M., Fisher Jr., W., Stingelin, R.W., 1968. Detection, delineation and monitoring of subsurface coal fires by aerial infrared scanning. Geographer HRB-Singer, Inc., a subsidiary of the Singer Company, state College, Pennsylvania, USA, pp. 877–881.

Kuenzer C., 2005. Demarcating coal fire risk areas based on spectral test sequences and partial unmixing using multi sensor remote sensing data. Ph.D. thesis, Technical University Vienna, Austria, 199 pp.

Kuenzer C., Voigt S., 2003. Vegetationsdichte als moeglicher Indikator fuer Kohlefloezbraende? Untersuchung mittels Fernerkundung und GIS. In: Strobl, J., Blaschke, T., Griesebner, G., (eds.), Angewandte Geographische Informationsverarbeitung XV. Beitraege zum 15. AGIT-Symposium Salzburg 2003. –Heidelberg, Wichmann, 256–261.

Kuenzer, C., Zhang, J., Hirner, A., Bo, Y., Jia, Y., Sun, Y., 2005. Multitemporal in-situ mapping of the Wuda coal fires from 2000 to 2005 — assessing coal fire dynamics. Proceedings of the International Conference on Coal Fire Research, 29.11.-01.12.2005 Beijing, pp. 104–106.

Kuenzer, C., Zhang, J., Tetzlaff, A., Voigt, S., Van Dijk, P., Wagner, W., Mehl, H., 2007a. Uncontrolled coal fires and their environmental impacts: investigating two arid mining environments in north-central China. Applied Geography vol. 27, 42–62.

Kuenzer, C., Zhang, J., Li, J., Voigt, S., Mehl, H., Wagner, W., 2007b. Detection of unknown coal fires: synergy of coal fire risk area delineation and improved thermal anomaly extraction Accepted for publication at International Journal of Remote Sensing. doi:10.1080/01431160701250432.

Kuenzer, C., Hecker, C., Zhang, Wessling, S., Wagner, W., 2007c. The potential of multi-diurnal MODIS thermal bands data for coal fire detection Accepted for publication at: International Journal of Remote Sensing. doi:10.1080/01431160701352147.

Kuenzer, C., Wessling, W., Zhang, J., Litschke, T., Schmidt, M., Schulz, J., Gielisch, H., Wagner, W., 2007d. Concepts for green house gas emission estimation of underground coal seam fires. Geophysical Research Abstracts of the EGU General Assembly 2007, 16.4.-20.4. Vienna, Austria, 2. pp.

Lapham, D.M., Barnes, J.H., Downey, W.F., Finkelman, R., 1980. Mineralogy associated with burning anthracite deposits of Eastern Pennsylvania. Mineral Resource Report 78 of the Pennsylvania Geological Survey, 82. pp.

Li, D.X., 1985. Applied study of airborne remote sensing in Taiyuan coalfield, China. Internal Report of the Remote sensing centre of the ministry of coal industry, Xian, China, 3–10 (in Chinese).

Litschke, T., Wiegand, J., Schloemer, S., Gielisch, H., Bandelow, K.F., 2005. Detailed mapping of coal fire sites in combination with in-situ flux measurements of combustive gases to estimate gas floor balance and fire development. Proceedings of the International Conference on Coal Fire Research, 29.11.-01.12.2005 Beijing, pp. 161–163.

Livingood, M., Winicaties, J., Stein, J., 1999. Centralia mine fire analysis: presence of sulfur-bearing mineral deposits at thermal vents. Research paper at West Chester University, Pennsylvania, USA. 9 pp.

Lohrer, C., Schmidt, M., Krause, U., 2005. Influence of environmental parameters on the self ignition of coal. Proceedings of the International Conference on Coal Fire Research, 29.11.-01.12.2005 Beijing, pp. 110–112.

Mansor, S.B., Cracknell, A.P., Shilin, B.V., Gornyi, V.I., 1994. Monitoring of underground coal fires using thermal infrared data. International Journal of Remote Sensing vol. 15 (8), 1675–1685.

Masalehdani, M.N., Potdevin, J.L., Cazier, F., Courcot, D., Paquette, Y., 2005. Coal waste heap fires – emission of toxic gases and condensation minerals, Northern France measurements and analyses. Proceedings of the International Conference on Coal Fire Research, 29.11.-01.12.2005 Beijing, pp. 101–103.

Moxham, R.M., Greene, G.W., 1967. Infrared surveys of coal mine fires in the anthracite and bituminous fields, Pennsylvania. USA, Geological Survey Inter-Agency Report BM-2, 67. U.S. Bureau of Mines.

Pennig L., 2003. Vergleich zweier Kohlebrandregionen in Nordchina mit Hilfe von Fernerkundungs-daten und GIS. Master Thesis at the University of Jena, 90 pp.

Prakash, A., Gupta, R.P., 1998. Land-use mapping and change detection in a coal mining area – a case study in the Jharia coalfield, India. International Journal of Remote Sensing vol. 19 (3), 391–410.

Prakash, A., Gupta, R.P., 1999. Surface fires in Jharia Coalfield, India — their distribution and estimation of area and temperature from TM data. International Journal of Remote Sensing vol. 20 (10), 1935–1946.

Prakash, A., Saraf, A.K., Gupta, R.P., Dutta, M., Sundaram, R.M., 1995. Surface thermal anomalies with underground fires in Jharia coal mine, India. International Journal of Remote Sensing vol. 16 (2), 2105–2109.

Rathore, C.S., Wright, R., 1993. Monitoring environmental impacts of surface coal mining. International Journal of Remote Sensing vol. 14 (6), 1021–1042.

Rosema, A., Guan, H., Veld, H., Vekerdy, Z., Ten Katen, A., Prakash, A., 1999. Manual of coal fire detection and monitoring. Netherlands Institute of Applied Geosciences (Report NITG 99-221-C, ISBN 90-6743-640-2), Utrecht, Netherlands (240 pp.).

Saraf, A.K., Prakash, A., Sengupta, S., Gupta, R.P., 1995. Landsat-TM data for estimating ground temperature and depth of subsurface coal fire in the Jharia coal field, India. International Journal of Remote Sensing vol. 16 (12), 2111–2124.

Schmugge, T.J., Becker, F., Li, Z.L., 1991. Spectral emissivity variations observed in airborne surface temperature measurements. Remote Sensing of Environment vol. 35 (No. 2), 95–104.

Schneider, W., 1996. The coal-bearing Jurassic at the southern margin of the Junggar basin, Xinjiang. Geowissenschaften vol. 14, 285–287.

Sun, Y., 2003. Personal Interviews during the fieldwork campaign in September 2003. (Y. Sun is an engineer of the Wuda coal fire fighting department and leads the team on coal geology).

Tetzlaff, 2004, Coal fire quantification using Aster, ETM and Bird satellite instrument data. Ph.D thesis at the Ludwig Maximilians University Munich, Germany, 155 pp.

Van Genderen, J.L., Guan, H., 1997. Environmental monitoring of spontaneous combustion in the North China coalfields, 243. Enschede, Netherlands.

Walker, S., 1999. Uncontrolled fires in coal and coal wastes. International Energy Agency, IEA on Coal Research –London, Great Britain, 73 pp.

Wessling A., 2007. The investigation of underground coal fires - towards a numerical approach for thermally, hydraulically and chemically coupled processes. PhD thesis at the Westfälische Wilhelms University of Münster, 157 pp.

Wessling, S., Litschke, T., Wiegand, J., Schloemer, S., Kessels, W., 2005. Simulating dynamic subsurface coal fires and its real life applications. Proceedings of the International Conference on Coal Fire Research, 29.11.-01.12.2005 Beijing, 114−117.

Zhang J., 2004. Spatial and Statistical Analysis of Thermal Satellite Imagery for Extraction of Coal Fire Related Anomalies. PhD thesis at the Technical University Vienna, Austria, 166 pp.

Zhang, X., Zhang, J., Kuenzer, C., Voigt, S., Wagner, W., 2004. Capability evaluation of 3–5 μm and 8–12,5 μm airborne thermal data for underground coalfire detection. International Journal of Remote Sensing vol. 25 (No. 12), 2245–2258.

Zhang, J., Kuenzer, C., Tetzlaff, A., Oettl, D., Zhukov, B., Wagner, W., 2007. Thermal Characteristics of Coal Fires 2: Result of measurements on simulated coal fires Accepted for publication at: Journal of Applied Geophysics vol. 63, 135–148. doi:10.1016/j.jappgeo.2007.08.003.